CONF-761101--11

PREPRINT UCRL- 78173

Lawrence Livermore Laboratory

Tritium Removal from Air Streams by Catalytic Oxidation and Water Adsorption

A. E. Sherwood

June, 1976

This paper was prepared for submission to the 24th Conference on Remote Systems Technology, American Nuclear Society, Nov. 14-19, 1976, Washington, D.C.

TRITIUM REMOVAL FROM AIR STREAMS BY CATALYTIC OXIDATION AND WATER ADSORPTION*

A. E. Sherwood
Lawrence Livermore Laboratory
University of California
Livermore, California 94550

June, 1976

ABSTRACT

An effective method of capturing tritium from air streams is by catalytic oxidation followed by water adsorption on a microporous solid adsorbent. Performance of a burner/dryer combination is illustrated by overall mass balance equations. Engineering design methods for packed bed reactors and adsorbers are reviewed, emphasizing the experimental data needed for design and the effect of operating conditions on system performance.

*This work was performed under the auspices of the U.S. Energy Research & Development Administration, under contract No. W-7405-Eng-48.

INTRODUCTION

Releases to the environment from experimental facilities handling tritium must be maintained at very low levels to insure the safety of on-site personnel and to minimize any long-term biological effects on large population groups. Engineering design of air purification systems will become more difficult as the fusion power program proceeds towards research facilities handling tritium in large quantities.

Metal getter beds offer an attractive method of capturing tritium from an inert, oxygen-free environment. Tritium gas can subsequently be regenerated for reuse by heating the hydride. In the presence of air, however, oxide formation can quickly destroy getter efficiency and other trapping schemes must be explored.

An effective method of capturing tritium from ventilation air or mixed gas waste streams is by catalytic oxidation followed by water adsorption on a microporous solid adsorbent. Burners and dryers have been used to purify air streams for many years. The purpose of this paper is to review engineering design methods, emphasizing design equations for packed bed catalytic reactors and adsorbers and the basic data needed for application to tritium control systems where high purification is required.

BURNER/DRYER OPERATION IN STEADY FLOW

Performance of a simple burner/dryer combination can be illustrated quantitatively from mass balance relationships in quasi-steady, once-through operation. The adsorption bed is inherently non-steady since water is

accumulation on the adsorbent. However, the outlet water vapor may be assumed to be in equilibrium, at mole fraction y_i, with the initially dry solid until break-through time is reached. An estimate of break-through time is given in a following section. We assume that the catalytic reactor is in a steady operating condition, converting a fixed fraction, $1 - \delta$, of inlet hydrogen to water. We neglect any isotopic selectivity during oxidation and adsorption. The terms hydrogen and water are used generically to refer to isotopic mixtures containing protium, deuterium, and tritium.

Figure 1 shows a schematic model of the situation we wish to illustrate: an air feed stream joining with a tritium contaminated deuterium gas stream. For this case, the dilution air flow rate is a design variable. This model represents the conceptual cleanup system for RTNS-II, the first of ERDA/DCTR's dedicated neutron source facilities.[1,2] The deuterium waste stream may contain small amounts of contaminants other than tritium gas but these are neglected here for simplicity.

Combining mass balances around reactor and adsorber leads to expressions for tritium effluent mole fractions as gas and water vapor, y^T and y_w^T, and tritium gas and water escape ratios, e^T and e_w^T. The results are:

$$y^T = \delta\, y_f^T \frac{Q_f}{Q} \quad , \tag{1}$$

$$y_w^T = (1 - \delta)\, \frac{y_i}{1 - y_i}\, \frac{1 - y_w}{y_w}\, y_f^T \frac{Q_f}{Q} \quad , \tag{2}$$

$$e^T = \delta \quad , \tag{3}$$

$$y_w^T = \left(1 - \frac{y_i}{1 - y_i}\right)\frac{1 - y_w}{y_w} \quad . \tag{4}$$

In the above, y_f^T is tritium gas mole fraction in the deuterium stream at flow rate Q_f. Mole fraction y_w represents water vapor at the reactor outlet.

$$y_w = \frac{y_{wf} R + 1 - \delta}{R + (1 + \delta)/2} \quad , \tag{5}$$

where R is the feed air/deuterium dilution ratio.

$$R = \frac{Q_{af}}{Q_f} \quad . \tag{6}$$

Effluent flow rate, Q, is given by,

$$Q = \frac{1 - y_w}{1 - y_i}\left[1 + (1 + \delta)/2R\right]Q_{af} \quad , \tag{7}$$

and the water accumulation rate on the solid adsorbent is,

$$Q_{ws} = \frac{1 - y_i/y_w}{1 - y_i}\left[y_{wf}R + 1 - \delta\right]Q_f \quad . \tag{8}$$

The above equations are exact, for the stated assumptions, since the Q's are volume flow rates at arbitrary standard conditions and thus represent mass flow rates. To simplify the algebra, we further assume that

for typical operating conditions [illegible] and R [illegible] 1

[illegible] and (7) then reduce to:

$$[illegible] \qquad (9)$$

$$Y_w \approx Y_f \frac{Y_{wf}}{Y_{wf}R + 1} \qquad (10)$$

Tritium effluent concentration levels are important in [illegible] applications when the air is returned to a laboratory room or fusion reactor hall.[3]

If the effluent is to be released through a ventilation stack, concentration levels are irrelevant. Curie emission rates are the crucial design variables since they become the source terms for a stack dispersion calculation. Emission rates for tritium as gas or water vapor are obtained directly from the escape ratios, Eqs. (3) and (4), by multiplying by the *curie feed rate*.

For the neutron source facility to be constructed at LLL, RTNS-II, tritium evolution from titanium tritide targets may approach 10^3 Ci/d. If, for discussion purposes, we specify gas and water emission rates of $\leq$ 1 Ci/d, then escape ratios must be $\leq 10^{-3}$. For those who prefer large numbers, the reciprocal of escape ratio is the decontamination factor, sometimes euphemistically referred to as purification factor. From the tritium gas escape ratio, Eq. (3), we see that the hydrogen fraction unconverted in the reactor must be $\leq 10^{-3}$, i.e., better than 99.9 conversion is required. Design factors influencing reactor conversion are discussed in the next section.

The tritiated water escape ratio and the adsorbed water accumulation rate are interrelated. For the simplifying assumptions stated above, Eqs. (4) and (8) become:

$$e_w^T = y_i \frac{R}{y_{wf}R + 1} \quad , \tag{11}$$

$$Q_{ws} = Q_f(y_{wf}R + 1) \quad . \tag{12}$$

To achieve a low water escape ratio requires an efficient adsorbent ($y_i << 1$). For a given adsorbent, y_i may be reduced, if necessary, by operating the bed below ambient temperature or by regeneration at higher bed temperature. For 5A molecular sieve at ambient temperature, an approximate value is $y_i = 10^{-6}$.

One would also like to keep the contaminated adsorbed water generation rate to a minimum and thereby ease handling problems if the spent adsorbent is to be disposed of by encapsulation and burial. Equation (12) then tells us to use dry dilution air ($y_{wf} = 0$). Dry air is also desirable to maintain a highly concentrated waste stream if the contaminated water is slated for a tritium recovery process.

For the dry air case,

$$e_w^T = y_i R \quad ,$$

$$Q_{ws} = Q_f \quad .$$

[illegible]

The air dilution ratio is not necessarily a variable controlled by the designer. The contaminated stream may arrive for processing in a highly dilute form. For RTNS-II, the primary waste stream is a small deuterium flow, essentially air free. However, there are other relatively high flow rate streams containing small amounts of tritium contamination which may have to be processed. For high air dilution, water vapor can be added to the inlet stream. For moist air, when R is very large, Eqs. (11) and (12) become,

$$\epsilon_w^* = \frac{f_s}{y_{wf}} \quad ,$$

$$\hat{y}_{wt} = y_{wf}\hat{y}_f R + y_{wf}\hat{y}_{af} \quad .$$

If the inlet air is water saturated, y_{wf} = 0.03 and the tritiated water escape ratio is about the same as the dry air case with R = 30. The waste water accumulation rate may, however, increase by orders of magnitude for high air flows.

PACKED BED CATALYTIC REACTOR

A packed-bed reactor often consists simply of a cylindrical tube filled with porous solid pellets as sketched in Fig. 2. The pellets provide

a large surface area to catalyze reaction as fluid moves through the tube. Beek & Bertje[5,6,7] ... equally starts from a pseudo-continuum model which ignores detailed hydrodynamic flow patterns on the particle scale, and assumes that field variables (concentration and temperature) can be represented by suitable local average values. Mass conservation for a fluid-phase species with local concentration, c, is written,

$$\frac{\partial}{\partial t}(\varepsilon c) + \nabla \cdot (c\vec{u} - D\nabla c) = r \quad , \qquad (13)$$

where ε is bed porosity, $\vec{u}$ is the superficial velocity vector, D is a dispersion coefficient, and r is a pseudo-homogeneous generation rate accounting for chemical reaction on the solid surface.

The equation for energy conservation is similar in form to the above, and temperature and concentration fields are generally strongly coupled by reaction heat effects, thereby complicating reactor design. Typical reactor temperature contours are shown in Fig. 1. The importance of temperature effects can be estimated from the equation for adiabatic temperature rise:

$$\Delta T = \frac{(-\Delta H) c_y}{\rho c_p} \quad ,$$

where ΔH is the reaction enthalpy change, c_y is the reactant feed concentration, and ρ, and c_p are fluid density and heat capacity. Hydrogen oxidation is highly exothermic (57.8 kcal/mol) and the above equation predicts an 80°C maximum temperature rise for a mixture containing only 1% hydrogen in air. To make the discussion simpler, we will assume the reactor is isothermal,

which implies that the contaminated waste stream is very dilute in hydrogen or other combustibles.

For an isothermal reactor, Eq. (13) is more tractable since radial concentration gradients are minimal if temperature gradients are absent. If particle size is much smaller than tube diameter, it is reasonable to assume a flat velocity profile across the tube and radial concentration gradients vanish by this assumption. Assuming steady operation, Eq. (13) then reduces to,

$$0 = -u\frac{dc}{dz} + D\frac{d^2c}{dz^2} + r \quad , \tag{14}$$

where z is the axial coordinate.

The axial dispersion coefficient, D, is much larger than a molecular diffusion coefficient and reflects interstitial mixing effects that are not explicitly included in a pseudo-continuum model. In a first approximation[8]

$$D = \frac{1}{2} d_p u \quad , \tag{15}$$

where d_p is the particle diameter. Neglect the dispersion term for the moment and assume a first order irreversible reaction,

$$r = -kc \quad . \tag{16}$$

Integration of Eq. (14) then gives, assuming constant fluid density, the fraction of reactant unconverted in a reactor of length L,

$$\frac{c}{c_0} = e^{-kL/u} \quad . \tag{17}$$

or, since L/u is the residence time in the reactor,

$$\cdot e^{-KV/Q} \quad . \tag{18}$$

where V is reactor volume. For fixed flow rate, Q, Eq. (18) implies that conversion is independent of reactor shape for a given volume. One would like a large cross-section and a short reactor length to minimize pump size and energy consumption. Dispersion limits conversion, however, in a short reactor. Equation (14) can be solved without neglecting the dispersion term[9] and the fraction unconverted, c', may be compared to the plug flow (no dispersion) case for the same reactor volume. If D/uL is small, the result[10] is,

$$c' = 1 + \left(\frac{KL}{u}\right)^2 \frac{D}{uL} \quad . \tag{19}$$

Substituting Eq. (15) and (17) into (19) gives,

$$c' = 1 + (4\pi)^2 \frac{d_p}{2L} \quad . \tag{20}$$

The minimum reactor length is often taken[8] to be 100 d_p. For $\epsilon = 10^{-3}$, Eq. (20) gives $c' = 1.24 \times 10^{-3}$ and the error in neglecting dispersion is larger if higher conversion is required.

The dominant factor influencing conversion is the overall rate coefficient, K, which has been defined in Eq. (16) as the proportionality constant in a first-order rate equation. Experimental work of Belovodskii et al.[11] on tritium oxidation at 0.1-100 ppm feed concentration levels

indicates that first-order kinetics is not obeyed with conversion decreasing at lower feed concentrations. For this discussion, we will assume that reaction rate is linear in concentration. Rate coefficient, K, is a lumped parameter representing a pseudo-homogeneous reaction occurring in a local volume element of the packed bed and must be related to the kinetic rate on the solid surface. In order to enhance reaction rate, catalyst particles generally have a high specific surface area (10^2 m^2/g or higher) and therefore intraparticle pore diffusion influences the overall rate. There may also be mass transfer limitations due to boundary-layer diffusion in the fluid phase exterior to the particle. Figure 4 sketches the progress of the reactant from bulk fluid to the catalytic surface.

A quantitative expression for the rate coefficient can be obtained by solving the steady diffusion/reaction equation within the porous particle with a surface flux boundary condition.[12,13] For a spherical particle, the result is,

$$K = \eta k_m (1 - \epsilon) \quad , \tag{21}$$

where η is called the catalyst effectiveness factor,

$$\eta = \frac{3}{\phi^2} \frac{\phi \coth \phi - 1}{1 + \frac{2D_e}{k_m d_p} (\phi \coth \phi - 1)} \quad , \tag{22}$$

and ϕ, referred to as the Thiele parameter, is defined by

$$\phi = \frac{d_p}{2} \sqrt{\frac{\bar{k}}{D_e}} \quad . \tag{23}$$

Although derived for spherical particles, Aris[13] has shown that the equations can be used for arbitrary particle shape if an equivalent spherical pellet is defined having the same external surface area to volume ratio. In the equations above, k is the specific rate coefficient for a heterogeneous fluid-surface reaction, · is the catalyst particle internal surface area per unit volume, D_e is the effective diffusivity within the pore structure, and k_m is the mass transfer coefficient at the fluid-particle interface.

The surface kinetic rate coefficient is generally strongly temperature dependent and simple approximations to Eq. (21) apply in various temperature regimes. At low temperature ($\phi \ll 1$):

$$K = k \cdot (1 - \epsilon) \quad . \tag{24}$$

At intermediate temperatures ($\phi \gg 1$, $\sqrt{k \cdot D_e} \ll k_m$):

$$K = \frac{6}{d_p} \sqrt{k \cdot D_e} \quad (1 - \epsilon) \quad . \tag{25}$$

At high temperature ($\phi \gg 1$, $\sqrt{k \cdot D_e} \gg k_m$):

$$K = \frac{6}{d_p} k_m (1 - \epsilon) \quad . \tag{26}$$

Practical operating conditions are often in the lower temperature range where the fluid-particle mass transfer coefficient has only a small effect on the overall rate and a rough estimate of k_m is sufficient. Correlations of packed-bed data are available[8,14] over a wide range of fluid properties

and particle Reynolds number. At low Reynolds number ($< 10^{1}$) $k_m \sim u$, and at high Reynolds number, $k_m \sim u^{\frac{1}{2}}$. A rough approximation is:

$$k_m = 0.3u \quad . \tag{27}$$

The effective pore diffusivity will have an important effect on the overall rate coefficient at intermediate temperatures as shown by Eq. (25) Catalyst pellets typically have pores in the 20-100 angstrom size range where Knudsen diffusion prevails and $D_e \sim T^{\frac{1}{2}}$. For alumina pellets[6,15] with deuterium diffusing in air, D_e can be approximated by,

$$D_e(m^2/s) = 4 \times 10^{-8} \sqrt{T(K)} \quad . \tag{28}$$

The kinetic rate coefficient must be determined experimentally for any selected catalyst. Proven commercial catalysts[16] for removing hydrogen from air streams are the platinum group, and copper oxide or a CuO/MnO_2 mixture called Hopcalite. Both Pt and Hopcalite catalysts are in use for tritium removal.[17,18,19] The Pt group catalysts may be inhibited or poisoned by halogen compounds, sulfur, heavy metals, CO, and lubricating oils. Hopcalite is much less sensitive to feed stream impurities[20] but is not as effective as Pt at moderate temperatures.[21]

There are very little data available on kinetic rate coefficients for the precious metal catalysts. Bixel and Kershner[18] measured tritium oxidation rates with Pt supported on $3.18\ 10^{-3}$m (1/8 inch) alumina particles at two temperatures. They assumed that pore diffusion was unimportant and fit k_r directly to an Arrhenius equation,

$$k_r = ae^{-E/RT} \quad . \tag{29}$$

We prefer to use Eq. (21) with pore diffusion estimated by Eq. (28), in which case the constants in Eq. (29) are found to be,

$$a = 2.4 \times 10^9 \ s^{-1} \quad ,$$

$$E = 12.3 \ kcal/mol \quad .$$

Figure 5 shows calculated hydrogen fraction unreacted in a Pt/Al_2O_3 catalyst bed at various operating conditions, based on parameter values estimated above. At a given operating temperature, conversion is enhanced by increasing residence time. For fixed flow rate, this must be balanced against increased catalyst and pumping costs. Pumping costs are reduced at lower bed velocity, but mass transfer and dispersion limitations will then reduce conversion.

ADSORPTION BED DYNAMICS

The continuum model approximations discussed above for a packed bed reactor also apply to an adsorption bed packed with small pellets, and Eq. (13) is the applicable fluid phase mass conservation relation. We will again assume isothermal operation and neglect radial gradients, although temperature effects can be significant due to the heat of adsorption of water vapor; e.g., ~ 18 kcal/mol on 5A molecular sieve.[22] For adsorption beds, the reaction rate in Eq. (13) represents the water accumulation rate on the adsorbent surface and with axial dispersion neglected, Eq. (13) becomes,

$$\frac{\partial c}{\partial t} = -u \frac{\partial c}{\partial z} + (1 - \varepsilon) \frac{\partial q}{\partial t} \quad , \qquad (30)$$

where q is water concentration in the particle phase. The adsorbent will eventually become water saturated, and the accumulation rate equation must reflect the reversible nature of the adsorption process. Assuming a second-order surface reaction,

$$\frac{\partial q}{\partial t} = k_a[c(Q_a - q) - q/K_a] \quad . \tag{31}$$

where k_a is the adsorption rate coefficient, and Q_a and K_a are constants in a Langmuir equilibrium isotherm. The form of the Langmuir equation follows by setting $\frac{\partial q}{\partial t} = 0$ in Eq. (31):

$$q = \frac{Q_a K_a c}{1 + K_a c} \quad . \tag{32}$$

The pair of equations (30) and (31) were first solved analytically by Thomas.[23] The solution is complicated and will not be presented here. It represents the slow movement of fluid and solid concentration "waves" through the bed.[24,25,26] Of primary importance for engineering design is the time required for concentration waves to reach the bed outlet; termed breakthrough time for adsorption, and regeneration time for desorption.

The shape of the adsorption breakthrough curve is strongly influenced by the shape of the equilibrium isotherm. For a linear isotherm [$K_a = 0$ in Eq. (32)], the breakthrough curve is spread out in time due to the finite adsorption rate as sketched in Fig. 6. If K_a is large, the isotherm has a convex shape, termed favorable for the adsorption cycle. The convex shape has a sharpening effect on the breakthrough curve and tends to counteract

the dispersive effect of a finite adsorption rate. To a good approximation, for convex isotherms, the breakthrough front is nearly a step-change with breakthrough time given by

$$t_b = \frac{K_a(Q_a - q_f)}{(1 + K_a c_f)} (1 - \epsilon)\frac{z}{u} \quad . \tag{33}$$

where q_f is initial water concentration on the adsorbent, and c_f is water vapor concentration in the feed stream. For 5A molecular sieve, for example, at ambient temperature with a water-saturated feed stream,

$$t_b = 8 \times 10^3 \frac{z}{u} \quad . \tag{34}$$

An asymtotic approximation[24,27] to the regeneration time, t_r, required to dry the adsorbent to a low concentration level is

$$t_r = K_a Q_a (1 - \epsilon) \frac{z}{u} \quad . \tag{35}$$

As shown by Garg and Ruthven,[27] the above is only a rough approximation unless the bed is very long so that equilibrium conditions prevail at the bed outlet. Bed temperature will normally be elevated during regeneration to reduce the Langmuir constant, K_a, and thereby reduce regeneration cycle time to the same range as the adsorption cycle time.

It should be emphasized that detailed performance calculations of adsorption bed dynamics require experimental data on equilibrium adsorption isotherms, and on rate coefficients at bed operating conditions. Selective

adsorption due to isotopic differences in normal, deuterated, and tritiated water should also be considered.

CONCLUSION

Performance of a catalytic reactor/adsorption bed combination for removing tritium gas from a waste stream has been discussed above, and engineering design methods for packed bed reactors and adsorbers have been briefly reviewed.

A burner/dryer system can be very effective for tritium capture, and additional experimental data are needed for the design of high performance recovery units.

NOMENCLATURE

c	fluid concentration, mol/m^3
d_p	particle diameter, m
D	dispersion coefficient, m^2/s
D_e	effective pore diffusivity, m^2/s
e^T	tritium gas escape ratio
e^T_w	tritiated water escape ratio
k	surface kinetic rate coefficient, m/s
k_a	adsorption rate coefficient, $m^3/mol \cdot s$
k_m	fluid-particle mass transfer coefficient, m/s
K	pseudo-homogeneous reaction rate coefficient, s^{-1}
K_a	adsorption isotherm constant, m^3/mol
L	reactor length, m
q	particle phase concentration, mol/m^3
Q	effluent flow rate, m^3/s
Q_a	adsorption isotherm constant, mol/m^3
Q_{af}	inlet air feed rate, m^3/s
Q_f	deuterium feed rate, m^3/s
Q_{ws}	water accumulation rate on solid adsorbent, m^3/s
r	pseudo-homogeneous reaction rate, $mol/s \cdot m^3$
R	feed air/deuterium flow ratio
t	time, s
T	temperature, K
u	superficial velocity, m/s
V	bed volume, m^3
y_i	equilibrium water vapor mole fraction at adsorber outlet
y_w	water vapor mole fraction at reactor outlet

Nomenclature (continued)

x_w water vapor mole fraction in waste feed

x_t tritium gas mole fraction in waste feed

x_t' tritium gas mole fraction in effluent

x_w' tritiated water vapor mole fraction in effluent

z axial coordinate, m

α hydrogen fraction unreacted in oxidizer

ε packed bed void fraction

η catalyst effectiveness factor

σ particle internal surface area / volume ratio, m^{-1}

ϕ Thiele parameter

REFERENCES

1. J. C. Davis, et al., Livermore Intense Neutron Source: Design Concepts, UCRL 76956, 1975.
2. J. C. Davis, The Livermore Neutron Source Program, UCRL 77809, 1976.
3. J. D. Lee, et al., Mirror Reactor Blankets, UCID 17083, 1976.
4. B. Lewis and G. von Elbe, Combustion, Flames and Explosions of Gases, 2nd. Ed., Academic Press, 1961.
5. K. G. Denbigh and J.C.R. Turner, Chemical Reactor Theory, 2nd. Ed., Cambridge University Press, 1971.
6. E. E. Petersen, Chemical Reaction Analysis, Prentice Hall, 1965.
7. H. Kramers and K. R. Westerterp, Elements of Chemical Reactor Design and Operation, Academic Press, 1963.
8. G. F. Froment, in Chemical Reaction Engineering, Adv. Chem. Series 109, Amer. Chem. Soc., 1972.
9. J. F. Wehner and R. N. Wilhelm, "Boundary Conditions of Flow Reactor," Chem. Eng. Sci., 6, 89, 1956.
10. O. Levenspiel, Chemical Reaction Engineering, J. Wiley, 1962.
11. L. F. Belovodskii, V. K. Gaevoi, V. I. Grishmanovskii, V. V. Andramanov, V. N. Demenyuk, and V. V. Migunov, "Removal of Tritium from the Gaseous Wastes from Nuclear Power Stations," Atomnaya Energiya, 38, No. 4, 217, 1975.
12. C. McGreavy and D. L. Cresswell, "A Lumped Parameter Approximation to a General Model for Catalytic Reactors," Can. J. Chem. Eng., 47, 538, 1969.
13. R. Aris, "On Shape Factors for Irregular Particles," Chem. Eng. Sci., 6, 262, 1957.
14. P. A. Nelson and T. R. Galloway, "Particle-to-Fluid Heat and Mass Transfer in Dense Systems of Fine Particles," Chem Eng. Sci, 30, 1, 1975.

15. C. N. Satterfield and T. K. Sherwood, *The Role of Diffusion in Catalysis*, Addison-Wesley, 1963.

16. D. J. Thomas, Catalytic Processes and Proven Catalysts, Academic Press, 1970.

17. J. F. Shinehammer and P. W. Lamberger, Tritium Control Technology, U.S. A.E.C. Report DASH-1769, 1973.

18. J. C. Bixel and C. J. Kershner, "A Study of Catalytic Oxidation and Oxide Adsorption for the Removal of Tritium from Air," Proc. 2nd Envir. Prot. Conf., U.S. A.E.C. Report WASH-1332, 1974.

19. J. L. Anderson, F. A. Damiano, and J. F. Masino, "Tritium Handling Facilities at the Los Alamos Scientific Laboratory," Proc. 23rd Conf. on Remote Systems Tech., Amer. Nuc. Soc., 1975.

20. J. M. Mezick and T. W. Williams, Ind. Eng. Chem. Prod. Res. Rev., 14, 284, 1975.

21. R. A. Johns, Chem. Eng. Prog. Symp. Ser. 62, No. 63, 81, 1966.

22. D. W. Breck, Zeolite Molecular Sieve, J. Wiley, 1974.

23. H. C. Thomas, "Heterogeneous Ion Exchange in a Flowing System," J. Amer. Chem. Soc. 66, 1664, 1944.

24. E. N. Lightfoot, R. J. Sanchez-Palma, and D. O. Edwards, in New Chemical Engineering Separation Techniques, Interscience, 1962.

25. S. Goldstein, "On the Mathematics of Exchange Processes in Fixed Columns," Proc. Roy. Soc. A219, 151, 171, 1953.

26. T. Vermeulen, "Separation by Adsorption Methods," in Adv. Chem. Eng., Vol. 2, Academic Press, 1958.

27. D. M. Garg and D. M. Ruthven, "Theoretical Prediction of Breakthrough Curves for Molecular Sieve Adsorption Columns," Chem. Eng. Sci 28, 791-799, 1973.

FIGURE CAPTIONS

Figure 1. Schematic of a burner/dryer combination in quasi-steady once-through operation.

Figure 2 Schematic representation of (a) packed-bed reactor or adsorber, and (b) continuum model systems. Sketch adapted from Lightfoot, et al.[24]

Figure 3. Temperature contours in a packed-bed catalytic reactor during SO_2 oxidation. Tube wall maintained at 200°C. Inlet flow at 350°C. Based on Denbigh.[5]

Figure 4. Movement of reactive species from bulk fluid stream to eventual reaction on catalytic surface.

Figure 5. Hydrogen fraction unreacted vs. temperature, residence time (V/Q), and velocity (u). Calculated for Pt/Al_2O_3 catalyst bed with $d_p = 3.18\ 10^{-3}$ m, $\epsilon = 0.4$.

Figure 6. Comparative sketch of (a) adsorption equilibrium isotherms, and (b) corresponding bed breakthrough curves during adsorption cycle.

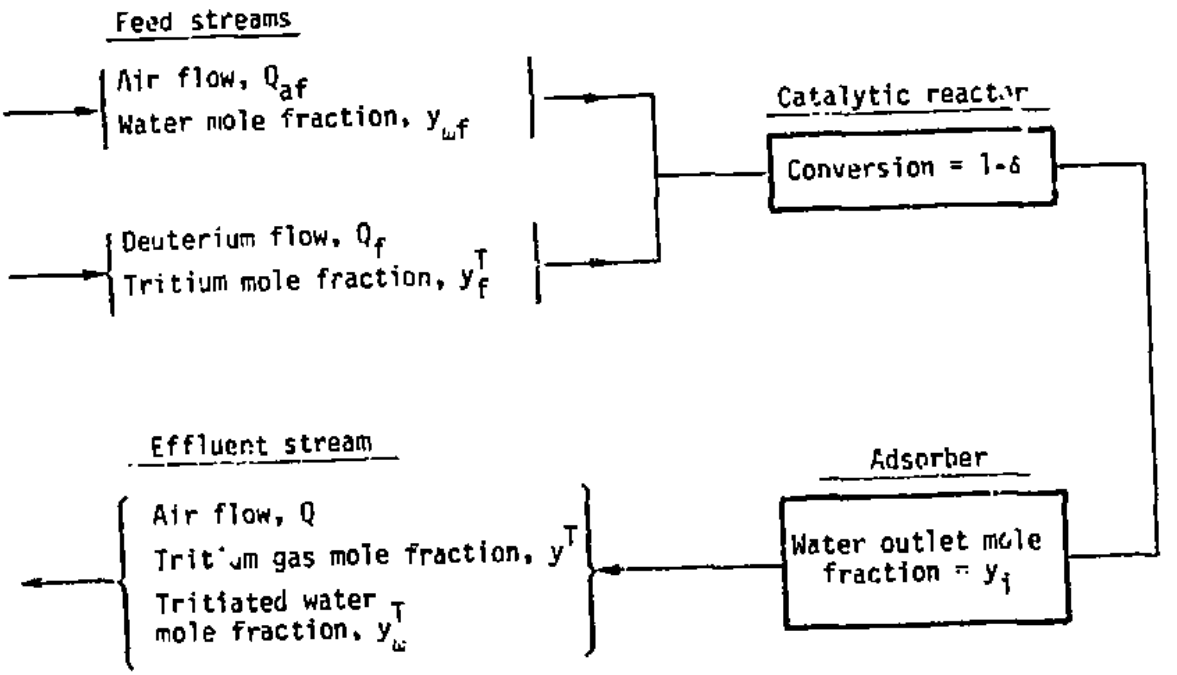
Feed streams
Air flow, Q_{af}
Water mole fraction, $y_{\omega f}$
Deuterium flow, Q_f
Tritium mole fraction, y_f^T
Catalytic reactor
Conversion = 1-δ
Adsorber
Water outlet mole fraction = y_i
Effluent stream
Air flow, Q
Tritium gas mole fraction, y^T
Tritiated water mole fraction, y_ω^T

Figure 1

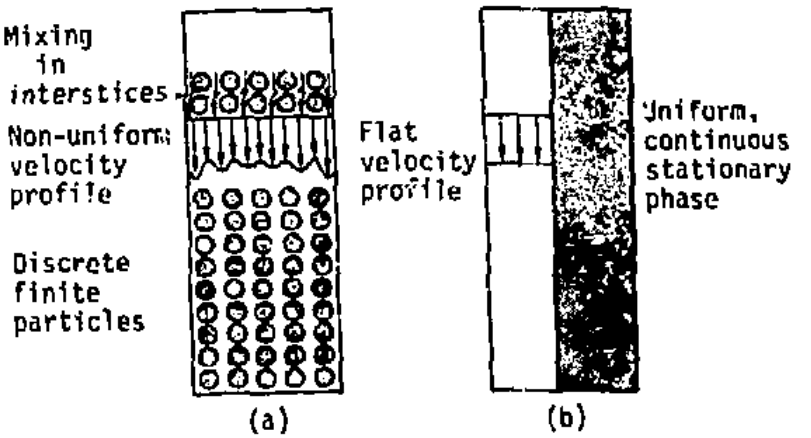
Mixing in interstices
Non-uniform velocity profile
Discrete finite particles
(a)
Flat velocity profile
Uniform, continuous stationary phase
(b)

Figure 2

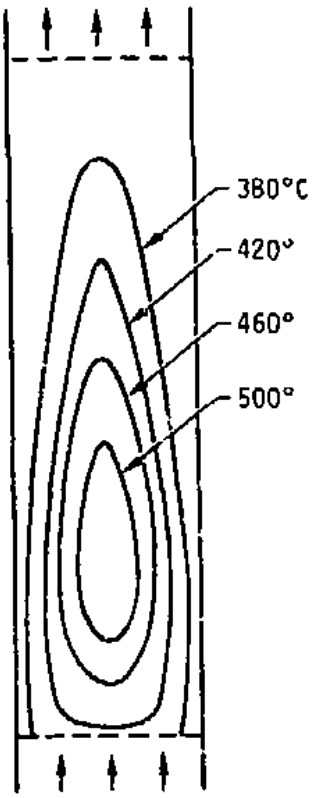

Figure 3

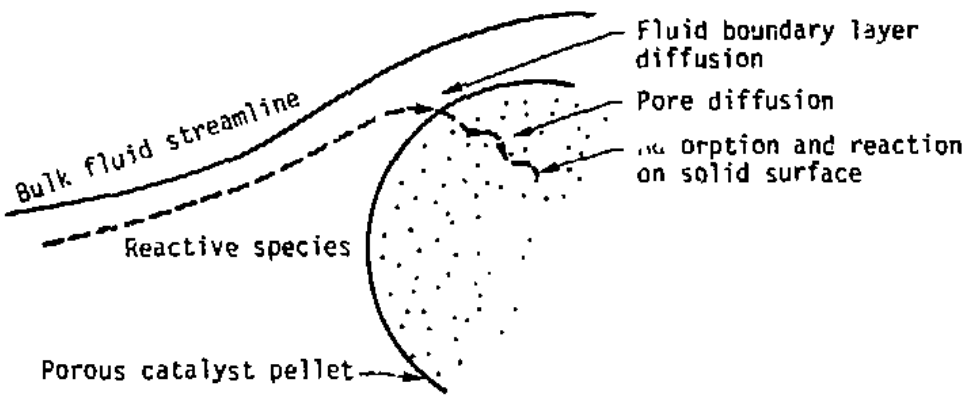
Fluid boundary layer diffusion
Pore diffusion
Adsorption and reaction on solid surface
Bulk fluid streamline
Reactive species
Porous catalyst pellet

Figure 4

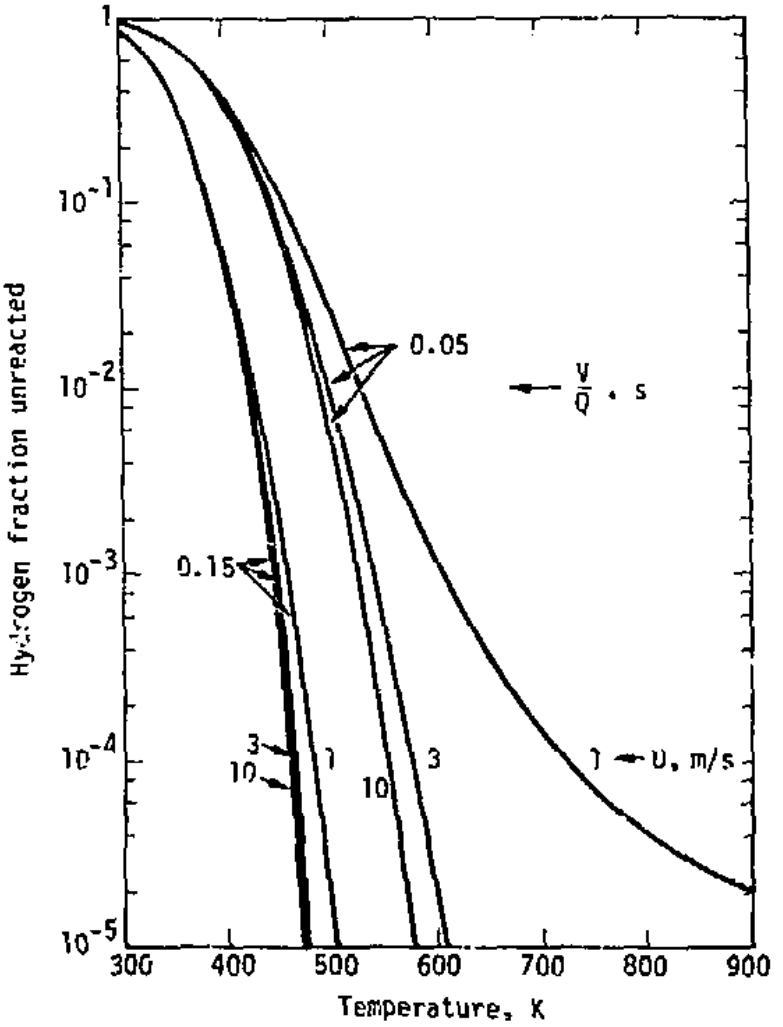
Hydrogen fraction unreacted
1
10^{-1}
10^{-2}
10^{-3}
10^{-4}
10^{-5}
0.05
$\frac{V}{Q}$, s
0.15
3
10
1
3
10
1
U, m/s
300
400
500
600
700
800
900
Temperature, K

Figure 5

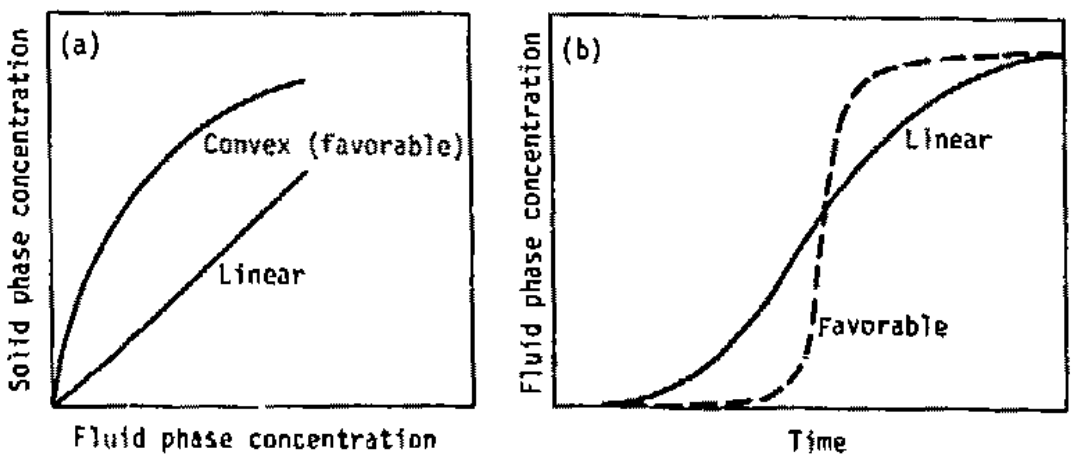
(a)
Solid phase concentration
Convex (favorable)
Linear
Fluid phase concentration
(b)
Fluid phase concentration
Linear
Favorable
Time

Figure 6